THE CLOSE-SEPARATION GRAVITATIONAL LENS CANDIDATE Q1009−0252[1]

PAUL C. HEWETT
Institute of Astronomy, Madingley Road, Cambridge CB3 0HA, United Kingdom
Electronic mail: pch@mail.ast.cam.ac.uk

MICHAEL J. IRWIN
Royal Greenwich Observatory, Madingley Rise, Cambridge CB3 0EZ, United Kingdom
Electronic mail: mike@mail.ast.cam.ac.uk

CRAIG B. FOLTZ
Multiple Mirror Telescope Observatory, University of Arizona, Tucson, Arizona 85721
Electronic mail: cfoltz@as.arizona.edu

MARGARET E. HARDING AND RUTH T. CORRIGAN
Institute of Astronomy, Madingley Road, Cambridge CB3 0HA, United Kingdom
Electronic mail: meh@mail.ast.cam.ac.uk, rtc@star.ph.lc.ac.uk

RACHEL L. WEBSTER
Department of Physics, University of Melbourne, Parkville, Victoria 3052, Australia
Electronic mail: webster@tauon.ph.unimelb.edu.au

NADINE DINSHAW
Steward Observatory, University of Arizona, Tucson, Arizona 85721
Electronic mail: ndinshaw@as.arizona.edu

Received 1994 May 4; revised 1994 June 21

ABSTRACT

We report photometry and spectra of three quasars, two of which make up a candidate close-separation gravitational lens, Q1009−0252A,B. The system is unusual in that a bright foreground quasar is projected only ~4.5 arcsec from the line of sight to Q1009−0252. The gravitational lens candidate consists of two images, magnitudes m_V=17.9 and 20.5, separation 1.53 arcsec. Spectra show both images to be quasars with redshift z=2.739 and very similar emission line and continuum properties, although the fainter component is somewhat redder and its emission lines have larger equivalent widths. CCD photometry in B, V, R and I confirms the fainter component has a redder $V-I$ color. Both components show strong Mg II absorption at z=0.869 and lensing by a massive galaxy at the absorption redshift can reproduce the main properties of the system. A second quasar, m_V=19.1, redshift z=1.627, lies only 4.62 arcsec from Q1009−0252A. The geometric and photometric properties we derive for the Q1009−0252 system are in good agreement with the results of Surdej *et al.* [Gravitational Lenses in the Universe: 31st Liege Int. Astroph. Coll. (Universite de Liege, Liege) (1994)], who discovered the system independently in the course of their ESO Key Project. Detection of weak absorption from the z=0.869 Mg II system in the z=1.627 quasar sets a lower limit to the scale of the Mg II absorber of $40h_{50}^{-1}$ kpc. Strong Mg II absorption is visible in both components of the lens candidate at the emission redshift of the nearby z=1.627 quasar, placing a lower limit of $45h_{50}^{-1}$ kpc to the size of the Mg II system associated with the quasar.

1. INTRODUCTION

We report here observations of a candidate for a gravitationally lensed quasar, Q1009−0252A,B and a close companion quasar Q1009−0252C. We identified the system as the result of a series of spectroscopic and photometric observations taken in 1990, 1992, and 1993. The system was subsequently discovered independently by the ESO Key Project team and photometry and spectroscopy of the system has been published by Surdej *et al.* (1994). Surdej *et al.* found the system to consist of two quasars, with identical redshifts, z=2.74, magnitudes m_B=18.2 and m_B=21.2, angular separation 1.55 arcsec, with a third quasar, redshift z=1.622, magnitude m_B=19.3, lying only 4.60 arcsec away. Strong metallic absorption systems were identified in the spectra of the close pair at redshifts z=0.866 and z=1.622. We describe our own observations that define the geometric and photometric properties of the Q1009−0252 system, which, while they differ in detail, are in good agreement with the properties derived by Surdej *et al.* In addition, we present high-quality spectroscopic data of all three components, including high-resolution observations of both metal absorp-

[1]Some of the observations reported here were obtained with the Multiple Mirror Telescope, a joint facility of the Smithsonian Institution and the University of Arizona.

 0004-6256/94/108(5)/1534/8/$0.90

tion systems, that allow interesting constraints to be placed on the spatial extent of the absorption systems. An explanation of the origin of the Q1009−0252 system in terms of gravitational lensing has much in its favor, but in a discussion of several explanations for the system we conclude that none provide an entirely satisfactory quantitative match to the observations.

Notwithstanding the considerable observational effort expended on surveys seeking gravitationally lensed quasars, the number of such systems identified remains small (e.g., Kochanek 1993). In an attempt to increase the number of known gravitationally lensed quasars, we are undertaking a study of the Large Bright Quasar Survey (LBQS) catalogue. The LBQS (Hewett *et al.* 1994) consists of more than 1050 quasars with redshifts $0.2 \leqslant z \leqslant 3.4$, and magnitudes $16 \leqslant m_{B_J} \leqslant 18.85$. 887 quasars in the LBQS have redshifts $z > 0.5$ and this subset forms the catalogue in which the incidence of both strong (multiply imaged quasars) and weak (possible excess numbers of close associations between quasars and foreground galaxies) lensing has been investigated. The first candidate multiply imaged quasar from the survey, Q1429−0053, was reported by Hewett *et al.* (1989). One aim of the LBQS survey was to provide a large well defined sample of apparently bright quasars for which the probability of detecting a multiply imaged quasar of specified configuration [number of images, angular separation(s), and magnitude difference(s)] could be calculated precisely. The techniques used to identify gravitational lens candidates from the APM scans of United Kingdom Schmidt Telescope (UKST) direct and objective-prism plates from which the LBQS was compiled are described in Webster *et al.* (1988) with an outline of their application to the LBQS sample given in Hewett *et al.* (1992). APM scans of UKST plate material provide an extremely effective method for identifying quasars and gravitational lens systems. However, it is difficult to obtain sufficiently accurate magnitude estimates of faint companion images located close ($\Delta\theta \leqslant 6$ arcsec) to LBQS quasars, and an extensive program of CCD imaging of all LBQS quasars with companions within $\Delta\theta < 10$ arcsec and magnitudes $m_{B_J} < 21.5$ has been undertaken. Sensitivity to close multiple quasar images with separation $0.3 \leqslant \Delta\theta \leqslant 3$ arcsec is also poor and CCD images in $\leqslant 1$ arcsec seeing of a sample of high-redshift, $z > 1.5$, high-luminosity, $M_{B_J} < -27.0$, LBQS quasars are also being obtained for detailed point-spread-function (PSF) modeling. Throughout this paper we use a value of $H_0 = 50$ km s^{-1} Mpc^{-1} and $q_0 = 0.5$, and define $h_{50} = H_0/50$ to indicate the scaling of linear sizes with the value of the Hubble constant.

2. OBSERVATIONS

The UKST B_J direct plate, J10147, shows Q1009−0252 as a stellar object, $m_{B_J} = 18.1$, with a second stellar image about 1.2 mag fainter visible ~5 arcsec north and west. Intermediate resolution spectra of both images were obtained at the Multiple Mirror Telescope (MMT) on the night of 1990 February 24. The brighter object was identified as a $z = 2.745$ quasar (reported in Hewett *et al.* 1991), and the fainter object as a $z = 1.627$ quasar. The Equinox B1950.0 coordinates of component A are $10^h09^m43.97^s$, $-02°52'12.0''$.

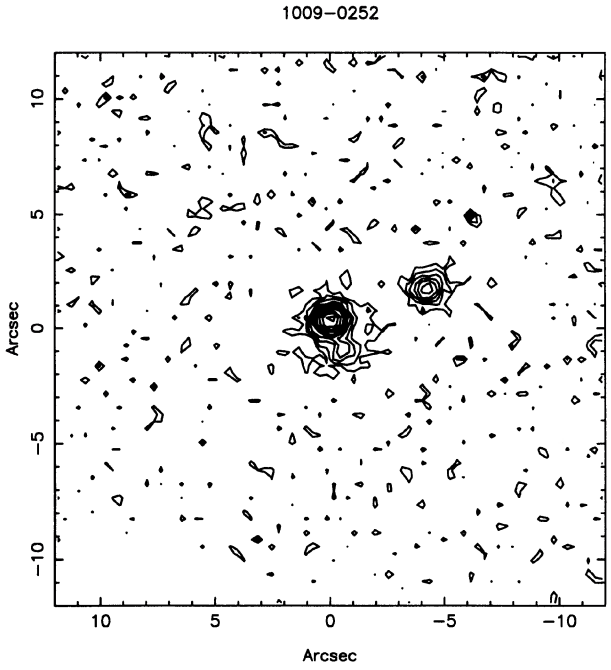

FIG. 1. Contour plot of a 20×20 arcsec region from the JKT I band frame of the Q1009−0252 system. Right ascension runs along the X axis, increasing to the left, and Declination along the Y axis, increasing to the top. The scale is in arcseconds on the sky and the plot is centered ($X=0$, $Y=0$) on component A. Component B can be seen at coordinates (−0.61,+1.41) and component C at (−4.39,+1.44). The small feature at (−6.7,+5.1) is a cosmic ray. The lowest contour level is set at a level of 1.5× the sky noise (σ_{sky}) in the CCD frame. The first contour corresponds to a surface-brightness level in the R band of ~24 mag per sq arcsec. The basic contour interval is also equal to $1.5\times\sigma_{sky}$. The second contour is at $3\times\sigma_{sky}$, thereafter, the contour level increases nonlinearly by a factor of 1.3 each time.

CCD imaging was obtained at the 0.9 m Jacobus Kapteyn Telescope (JKT) on La Palma on the night of 1992 April 1, through KPNO B, V, and I filters, and on the nights of 1992 November 1–4, through KPNO B, V, R, and I filters. On both occasions the detector was a 1242×1152 EEV CCD with a scale of 0.31 arcsec per pixel. Integration times were in the range 500–1200 s. Seeing conditions were good with measured full-width half-maximum values of 1.1 (B), 0.9 (V), and 0.8 arcsec (R and I). Conditions were photometric in the April run enabling magnitude zero points in B and V to be derived. The observations made in November were taken through light cirrus and no magnitude zero points were obtained.

Reductions were performed using IRAF[2] and included standard bias subtraction, trimming, and flatfielding operations using normalized twilight sky exposures. Visual inspection of the reduced frames, e.g., Fig. 1, showed the brighter image consists of two components. Magnitudes and positions

[2]IRAF is distributed by the National Optical Astronomy Observatories, which are operated by the Association of Universities for Research in Astronomy, Inc. under contract with the National Science Foundation.

TABLE 1. Q1009−0252 components—relative positions and magnitudes.

	δR.A. (″)	δDec. (″)	B	V	ΔB	ΔV	Δr	Δi
A	–	–	18.2	17.9	–	–	–	–
B	-0.59	-1.36	20.8	20.5	2.52 ± 0.20	2.62 ± 0.10	2.26 ± 0.10	2.03 ± 0.08
C	-4.39	1.44	19.3	19.1	0.93 ± 0.05	1.18 ± 0.02	1.16 ± 0.02	1.18 ± 0.02

for the two close components were derived using a PSF modeling technique (Irwin 1985). The model PSF was defined using isolated unsaturated stars within each CCD frame. Relative magnitudes and coordinates derived from the PSF-fitting procedure to the B, V, R, and I frames for all three components are given in Table 1. Zero-point magnitudes are also given for B and V. Components A and B have similar colors although B is definitely redder, with the magnitude difference Δm(A−B) decreasing systematically by 0.5 mag from the B band to the I band. Component C, the image of the $z=1.627$ quasar is bluer than both components A and B. No additional images were detected within a radius of 20 arcsec of component A to a limiting magnitude of $m_R \sim 21$. The three components A,B,C account for all the flux observed in the CCD frames of the system. In particular, there is no evidence of any underlying galaxy to a magnitude of $m_R \sim 21$.

Intermediate resolution (~5 Å) spectra of components A and B were obtained in conditions of 0.9 arcsec seeing at the 4.2 m William Herschel Telescope (WHT) on La Palma on 1993 April 9 using the ISIS double spectrograph. Red- and blue-arm observations were obtained concurrently giving a wavelength coverage of λλ3200–8500 Å. The spectra were wavelength calibrated using CuNe and CuAr arcs and flux calibrated using observations of the standard star Feige 34. In 0.9 arcsec seeing there was still significant overlap between the profiles of the two components along the slit. The spectrum of the bright component was extracted using the uncontaminated "half" of the profile furthest away from component B. By assuming profile symmetry we could extract component B by simply subtracting off the brighter component from the combined total spectrum. As a check on this result the spectra were also optimally extracted using only the least contaminated "half" of each components' profile. No significant differences resulted. We therefore conclude that the extraction has constrained the light contamination from the brighter component to be less than 10% of the total spectral flux derived for the faint component. This is born out by the marked difference in continuum slope between the two components. The spectra are shown in panels (a) and (b) of Fig. 2.

The spectra of images A and B show emission lines characteristic of high redshift quasars. The quasar redshift derived from the centroids of the principal emission lines is $z=2.739$. Gaussian fits to the peaks of the emission line profiles give wavelengths which are identical to within 2 Å (~150 km s^{-1}). There are, however, differences in the emission-line equivalent widths of the two spectra: Lyman

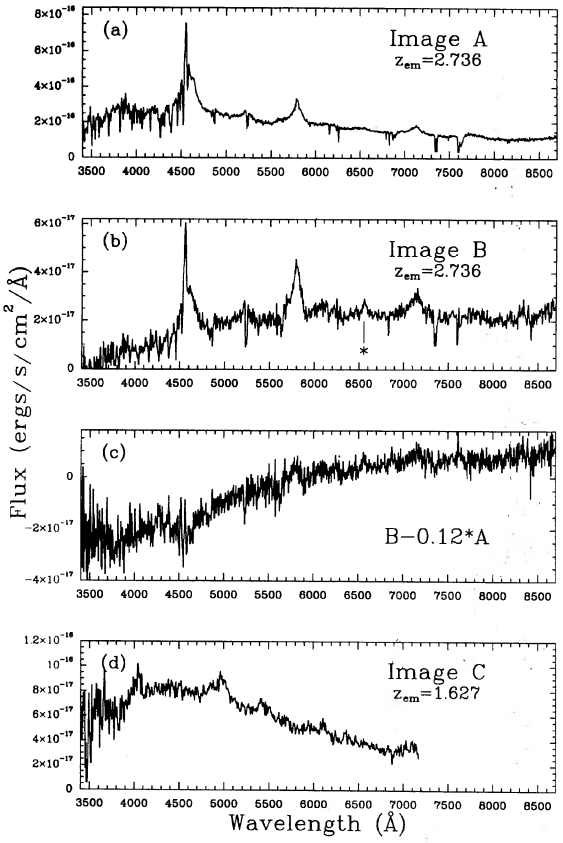

FIG. 2. Panels (a) and (b) show the WHT spectra of the components A and B obtained on the night of 1993 April 9. The resolution is ~5 Å. The spectra were obtained in conditions of 0.9 arcsec seeing (FWHM); the procedure employed to extract the individual spectra is described in the text. A feature at 6550 Å in the spectrum of B, possibly identifiable as [N III] λ1750, is marked with an asterisk. Panel (c) shows the result of subtracting a scaled version of the spectrum of A from B, with the Residual=B−0.12A. The residuals at the positions of the principal emission lines result from the different emission equivalent widths in the spectra of the two images. Note that some are positive and some negative, indicating that if variability is the cause of the differences, the lines do not vary in lockstep. The form of the residual spectrum on the large scale is indicative of the much redder spectral energy distribution of component B compared to component A. Note the lack of any continuum breaks, emission or absorption features that might indicate a contribution to the residual spectrum from any lensing galaxy. Panel (d) contains the MMT spectrum of component C, the redshift $z=1.627$ quasar. The spectrum has a resolution of ~10 Å and was obtained on the night of 1993 January 21. Emission from C IV λ1549, [C III] λ1909 is visible with strong Fe II multiplets also present.

α+N V λ1240 have a combined equivalent width of W_λ (Lyman α+N V)≃140 Å in A and 200 Å in B; W_λ (C IV λ1550)≃90 Å in A, 120 Å in B; and W_λ ([C III] λ1909)≃60 Å in A, 70 Å in B.

It is apparent from Fig. 2 that quasar B has a somewhat redder continuum slope than quasar A, consistent with the photometric color differences. This is shown explicitly in Fig. 2(c), where the residual flux following subtraction of a scaled spectrum of component A from component B (Residual=B−0.12×A) is shown. In addition to the large-scale difference in the continuum shapes, residual features at the wavelengths of Lyman α+N V, C IV, and [C III] are evident, confirming the difference in the equivalent widths deduced from the individual spectra. An emission feature at 6550 Å is also visible in the difference spectrum. The line at 6550 Å is seen in the spectrum of component B, equivalent width ~13±5 Å, with a somewhat sharper profile than the C IV λ1549 emission line. Component A may contain a weak, somewhat broader, feature at 6550 Å, but prominent emission with the narrower profile is present only in component B. At redshift $z=2.739$ the feature is coincident with the restframe wavelength of the [N III] λ1750 line. If the detection of strong emission at 6550 Å in component B alone is confirmed, it has important consequences for whether the Q1009−0252 system is a gravitational lens (Sec. 3). Also evident in both components are strong Mg II λλ2796,2803 (and associated Fe II) absorption systems at $z=0.869$ and $z=1.627$ with the lower redshift Mg II system appearing to be significantly stronger in the fainter quasar component [W_A(Mg II)≃6.6 Å vs W_B(Mg II)≃14.3 Å]. The two quasars also have a number of common absorption features blueward of the Lyman α emission line, in the region of the Lyman α forest, though the path length differences between the two lines of sight, irrespective of whether the quasar pair is a lens, are too small to set interesting limits on the sizes of the absorbers.

Figure 2(d) shows the spectrum of Q1009−0252C, obtained with the MMT on 1993 January 21. Although the emission lines are weak, C IV and [C III] lines are clearly present, as is Mg II which appears at the red end of the spectrum. Additional spectra of components A and B combined and component C were obtained at the MMT on the night of 1993 April 29 and 1994 January 19. The high signal-to-noise ratio, 2.2 Å resolution spectra which cover λλ4700–5600 Å and λλ6500–8100 Å are shown in Figs. 3 and 4. The Mg II λλ2796,2803 absorption, at $z=0.8688$ and $z=1.6266$, evident in the WHT spectra of A and B, is seen along with a number of additional features in the spectrum of A+B. The wavelengths, equivalent widths, and identifications of the absorption lines are given in Table 2. The $z=0.8688$ system is also seen, albeit weakly, in quasar C, suggesting the system is at least $40h_{50}^{-1}$ kpc in extent. The $z=1.6266$ system seen in A and B is, within the uncertainty of determining the emission redshift (σ_v≃600 km s^{-1}), at the identical redshift to quasar C. The higher redshift absorption system thus provides direct evidence for a structure of at least $45h_{50}^{-1}$ kpc associated with the quasar C.

Surdej *et al.* (1994) have published spectra of the three components of the system. Our spectra are of rather higher signal-to-noise ratio and extend slightly further to the blue and red. There is good agreement in the overall continua shapes, emission line strengths and profiles, and presence of the strongest intervening absorbers. The higher-resolution MMT spectra, Figs. 3 and 4, of the two principal absorption systems provide a much more detailed census of the individual features—Table 2. Our detection of weak Mg II at $z=0.8688$ in component C is consistent with the higher quality of the spectra shown in Fig. 3. Figure 1 in Surdej *et al.* shows no evidence of the presence of an emission feature at 6550 Å in component B, the line tentatively identified as [N III] λ1750 above, although their spectrum is probably not inconsistent with the existence of such a feature. A higher signal-to-noise ratio spectrum of component B is required to confirm the reality of the putative 6550 Å line.

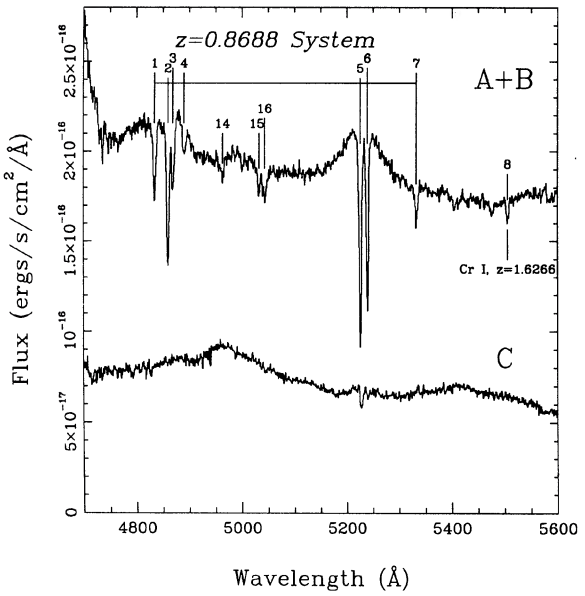

FIG. 3. MMT spectra of components A+B (combined) and component C showing the absorption features detected in the redshift $z=0.8688$ system that may signal the presence of a lensing galaxy at the same redshift. The numbering of the features corresponds to that adopted in Table 2 where the parameters of the individual absorption features are listed. The spectra have a resolution of 2.2 Å and were obtained on the night of 1994 January 19. Note that the flux scale and zero level is the same for both spectra.

Our measured separation of 1.53±0.01 arcsec between components A and B is in good agreement with the value of 1.55 arcsec determined by Surdej *et al.* The derived photometric properties for the system are also very similar. Surdej *et al.*'s zero-point magnitudes of components A and C in the B band are in excellent agreement ($\delta B<0.05$) with those in Table 1 and the relative magnitude differences A−B and A−C in the R and i bands also match—$\delta m<0.15$ in all cases. The only potentially significant difference between the datasets is the B band magnitude of component B. Our relative magnitude is $\Delta(A-B)_B=2.52$, whereas Surdej *et al.* find $\Delta(A-B)_B=3.0$. Formally, the difference is not significant, our quoted error is $\sigma=0.2$, and that of Surdej *et al.*, $\sigma=0.1$. We note that our measured value $\Delta(A-B)_B$ is very similar to that in the adjacent V band $\Delta(A-B)_V=2.62$, where Surdej

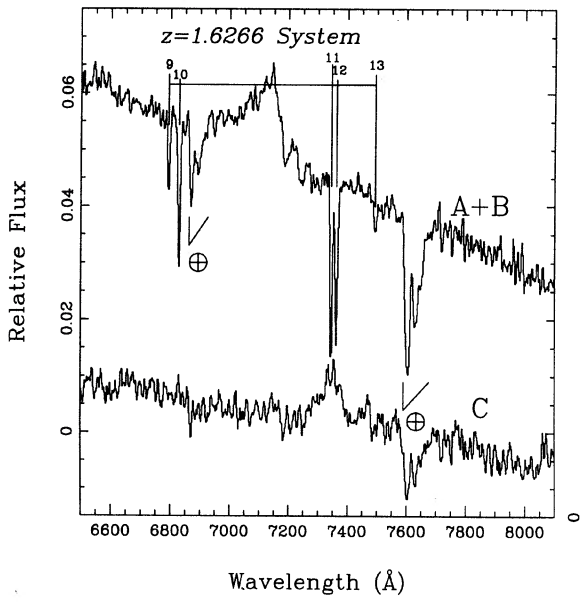

FIG. 4. MMT spectra of components A+B (combined) and component C showing the absorption features detected in the redshift $z=1.6266$ system that is coincident with the redshift of the quasar C. The detection of absorption in components A+B means the absorbing system associated with the quasar C is at least $45h_{50}^{-1}$ kpc in extent. The numbering of the features corresponds to that adopted in Table 2 where the parameters of the individual absorption features are listed. The spectra have a resolution of 2.2 Å and were obtained on the night of 1993 April 29. The flux scale is the same for both spectra but the zero flux level has been offset with the zero point of A+B indicated on the left abscissa and that for C on the right.

et al. have no data, and the flux ratio, integrated over a *B* band transmission profile, derived from the spectra of components A and B is consistent with the magnitude difference $\Delta(A-B)_B=2.52$.

3. DISCUSSION

Explanations for the properties of the Q1009−0252 system fall into two classes: the components A and B may be physically distinct quasars or the system represents the gravitational lensing of a single quasar by some intervening mass concentration. In the latter interpretation the differences in the continuum and emission line properties of the components may be due to one or more of four factors: (1) differential contribution to the flux associated with each quasar component from the lens itself, (2) differential extinction of the components by dust associated with the lens, (3) intrinsic variability of the lensed quasar on time scales comparable to the differences in light travel to the components, (4) differential microlensing by an intervening compact object, probably associated with the macrolens.

Examples of binary quasars are known to exist (Djorgovski *et al.* 1987) and several of the "dark" lenses with separations ~5 arcsec may be binaries. Under this hypothesis, Q1009−0252A,B are two quasars separated by only $\sim 11h_{50}^{-1}$ kpc in projection. Information on the amplitude of the spatial clustering of quasars on these scales is practically nonexistent. If the form of the quasar–quasar two-point correlation function observed at much larger

TABLE 2. Absorption lines in spectra of Q1009−0252 A+B and C.

	Wavelength (Å)	ID	Redshift	W_λ(A+B) (Å)	W_λ(C) (Å)	Notes
z=0.8688 system:						
1.	4834.06	Fe II λ2586	0.86885	1.22	< 0.3	$\sigma_{W(C)} \simeq 0.1$ Å
2.	4859.63	Fe II λ2600	0.8689	2.33	"	"
3.	4868.61	Fe II+MnII bl.		1.22	"	"
4.	4890.04	Fe II bl.		0.45	"	"
5.	5255.93	Mg II λ2796	0.86884	3.16	0.76	$\lambda(C) = 5257.90$
6.	5239.41	Mg II λ2803	0.86886	2.45	0.27	$\lambda(C) = 5240.29$
7.	5332.78	Mg I λ2853	0.8692	0.60	< 0.3	$\sigma_{W(C)} \simeq 0.1$ Å
z=1.6266 System[a] (note Zabs = Zem(C)):						
8.	5505.50	Cr I λ2096 bl.		0.37	"	$\sigma_{W(C)} \simeq 0.1$ Å
9.	6793.63	Fe II λ2586	1.62642	1.91	< 3	$\sigma_{W(C)} \simeq 1$ Å
10.	6829.30	Fe II λ2600	1.62648	4.38	"	"
11.	7345.56	Mg II λ2796	1.62680	6.52	"	"
12.	7363.27	Mg II λ2803	1.62640	6.79	"	"
13.	7494.70	Mg I λ2853	1.62698	1.33	"	"
Others:						
14.	4962.77	unidentified		0.32	< 0.3	$\sigma_{W(C)} \simeq 0.1$ Å
15.	5032.48	Mg II λ2796(?)	0.7992	0.41	"	"
16.	5043.08 bl	Mg II λ2803(?)	0.7992	0.86	"	"

[a]FeII 2344 and FeII 2383 absorption in this system seen in low-resolution data.

scales, with $r_0 \sim 12 h_{50}^{-1}$ Mpc, and slope ~ 1.8 (Shanks & Boyle 1994), extended to scales of tens of kiloparsecs, then the spatial clustering amplitude would be enhanced by a factor 10^5–10^6 over random, and the detection of such pairs in searches of many hundreds of quasars is not implausible. There is no necessity to explain the differences in the continuum and emission line properties; the observed differences are ascribed to intrinsically different emergent spectral energy distributions. Unfortunately, potentially the most significant difference between the spectra, the [N III] λ1750 emission line strengths, is the least well established from our data. Given the faintness of B relative to A, the apparent detection of the feature seen at 6550 Å cannot be established with total confidence, although we have examined the data carefully and can find no reason to question the presence of the feature. Detection of [N III] λ1750 emission is extremely rare in quasars (Osmer & Smith 1980; Osmer 1980), and coupled with its origin in a relatively extended broad line region, its presence in component B alone would present the gravitational lensing model for the system with severe difficulties. An advantage of the binary quasar model is that it does not conflict with any of the available evidence.

The gravitational lensing hypothesis also has substantial evidence in its favor. The strong, and spatially extended, absorption system at $z=0.869$ suggests the presence of a luminous galaxy at the same redshift (e.g., Drinkwater *et al.* 1993; Steidel 1992), and the angular separation and brightness of components A and B are consistent with lensing by a massive galaxy at the redshift of the absorption system. Consider a singular isothermal sphere (SIS) model: image separation 1.53 arcsec, component flux ratio 6.5 (taken from the *I* band), source redshift $z_{\rm source}=2.739$, and lens redshift $z_{\rm lens}=0.8688$. Then, the velocity dispersion is $\sigma=245$ km s^{-1}, with the lensing galaxy projected ~ 0.20 arcsec from component B, which is (de)magnified by a factor 0.36, while the light from component A, projected 1.33 arcsec on the other side of the galaxy, is amplified by a factor of 2.36. This geometry is consistent with the Mg II $z=0.8688$ system appearing to be strongest in component B if the absorption-line equivalent width is correlated with impact parameter (Lanzetta & Bowen 1990).

The SIS model places the component B very close on the sky to the lensing galaxy. The angular separation of the two quasar components is well determined and places tight constraints on the value of the velocity dispersion in the SIS model, $\sigma \sim 245$ km s^{-1}, and for a normal elliptical galaxy this velocity dispersion corresponds to an object with relatively low luminosity, $\lesssim L^*$. Unfortunately, the limiting magnitude for detection of a galaxy close to the quasar images from the existing CCD frames is relatively bright, $m_R \sim 21$. Even in the *R* band the *K* correction for an unevolved early-type galaxy at $z=0.87$ is large, ~ 1.8 mag (Coleman *et al.* 1980), and the present nondetection of a galaxy, which corresponds to an absolute magnitude limit of $M_R \gtrsim -24.5$, does not provide interesting constraints on the nature of any galaxy associated with the $z=0.869$ absorber.

A comparison of the spectra of components A and B confirms that the differences cannot be ascribed to the presence of an elliptical galaxy contributing only to the spectrum of component B. Specifically, an early-type galaxy at $z=0.869$ should not make a significant contribution to the flux in the *B*, *V*, and *R* bands, the 4000 Å break occurring at 7400 Å in the observed frame, and the emission-line equivalent widths of *B*, the component with the redder spectral energy distribution, are *larger* than in A, suggesting that the there is little additional light in the B spectrum. The residual spectrum resulting from subtraction of a scaled version of the spectrum of component A from the spectrum of B [Fig. 2(c)] supports this conclusion. The residual flux increases very strongly towards the red and the form is inconsistent with the continuum of any normal galaxy seen at a redshift of $z \sim 0.87$. Furthermore, there is no evidence for the presence of a 4000 Å break, *G* band, or other absorption features indicative of an early-type galaxy, and the lack of Ca II H & K absorption and any evidence of emission from [O II] λ3727 offers no support for identification of the spectrum with a galaxy of later type. The combination of the very red spectral energy distribution of the residual flux and the lack of any common absorption or emission features rules out the hypothesis in which the difference in the spectra of the two components is due to the presence of a normal galaxy.

An alternative explanation for the differences in the quasar continua is that the quasar images are undergoing differential extinction through the $z=0.869$ absorber. In this model a massive early-type spiral may be the lens. We have estimated the amplitude of the extinction required by assuming that image A is unreddened and B is extinguished by SMC-like dust at $z=0.869$. The (unreddened) shape of the continua of A and B are in good agreement if B suffers extinction of $E(B-V)=0.40\pm0.05$ mag (see Fig. 5). This implies a differential extinction of 1.6 mag in the observed-frame *I* band, leading to a true ΔI band magnitude of 0.43 mag or a flux ratio (A/B) of 1.5. A SIS lens model for this flux ratio and the observed separation places image A 0.92 arcsec on one side of the lensing galaxy and image B 0.61 arcsec on the other side, corresponding to impact parameters—$8.0 h_{50}^{-1}$ and $5.3 h_{50}^{-1}$ kpc, respectively. Thus, extinction by dust in the $z=0.869$ absorber can successfully reproduce the difference in the continuum shapes, although the differential extinction for two lines of sight at very similar impact parameters is perhaps rather large for comfort. More significantly, the extinction hypothesis does not address the differences in the equivalent widths of the prominent ultraviolet emission lines (which remain unaffected by the extinction), nor the presence in component B alone of the [N III] λ1750 emission line.

For flux ratios of 1.5 (intrinsic ratio in *I* band for differential extinction model described above) to 6.5 (observed *I* band) the simple SIS models for the lens predict time delays in the range ~30–100 days and intrinsic variations of the quasars continuum and emission line fluxes over this time scale provide a potential explanation for the differences in spectral energy distributions. Steidel & Sargent (1991) have argued that the significant differences in the emission line equivalent widths and profiles of two gravitational lens candidates, Q1634+267 and Q2345+007, result from intrinsic variability on time scales of months. To ascribe both the continuum and emission line differences between the com-

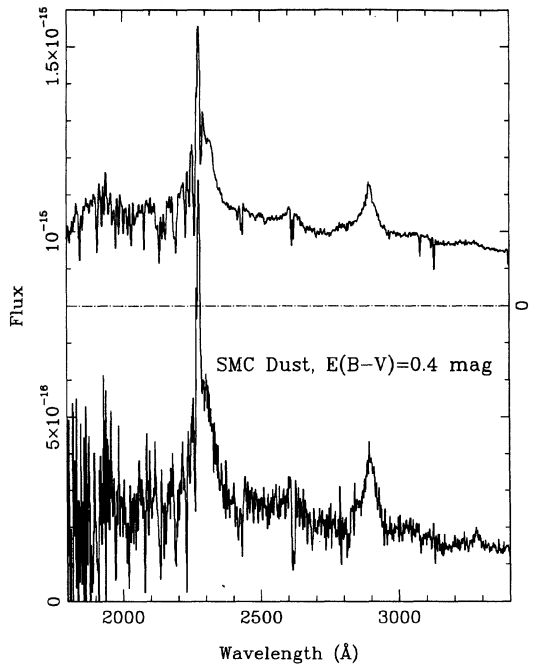

FIG. 5. WHT spectra of components A and B. The upper panel shows component A, as in Fig. 2(a). The lower panel shows the intrinsic spectrum of component B under the hypothesis that the observed spectrum has been affected by SMC-like dust in the $z=0.869$ absorber, giving a line-of-sight extinction of $E(B-V)=0.4$ mag. Note the very similar continuum shapes of A and B. The unreddened spectrum of B has been multiplied by a factor of 1.5 (see text) and the flux zero points have been offset with that for the top spectrum shown on the right abscissa. Telluric absorption is marked with ⊕.

ponents to intrinsic variations would make Q1009−0252 an extreme object and we are not aware of any recorded short time scale variation in the ultraviolet continuum of such a luminous quasar that has such a strong dependence on wavelength. Our knowledge of the characteristics of variability of luminous quasars is sparse (Maoz *et al.* 1994), but intrinsic variability is a possible explanation for the differences (or part thereof) in the emission line equivalent widths.

Microlensing by a compact object in the halo of the lensing galaxy at $z=0.869$, the third possible explanation for the difference in spectral energy distributions under the lensing hypothesis, is favored by Surdej *et al.* Surdej *et al.* suggest that the difference in the spectra of the components results from the effects of microlensing producing an excess of blue light in component A. Under this hypothesis, the relative amplification of the quasar continuum due to microlensing increases by ~60% over a rest-frame wavelength range of only ~700 Å. This implies an extremely strong dependence of the effective spatial extent of the continuum source as a function of wavelength. If microlensing is responsible for such a dramatic differential amplification, then interesting constraints on the scale of the continuum generating as a function of temperature may be derivable. The microlensing hypothesis is appealing in some ways, but we do not favor this explanation as the main source of the difference in spectral energy distributions. The spectral energy distribution of component A is typical for quasars, whereas that of B is somewhat red, providing circumstantial evidence against the microlensing hypothesis, although this is marginal at best.

To summarize, if the Q1009−0252 system arises through gravitational lensing then an explanation for the substantial differences in the form of the quasar spectral energy distributions is required. Intrinsic continuum/emission line variability or microlensing of component A are both technically possible, but Q1009−0252 would represent a very extreme situation if either explanation were responsible for the bulk of the differences in the observed spectral energy distributions. Differential extinction by dust in the lensing galaxy provides a very plausible explanation for the large-scale change in the quasar continuum shape. Combining the extinction model with a much less extreme element of intrinsic variability or degree of microlensing would allow the spectroscopic and photometric properties of the system to be reproduced. The sole caveat would then be the possible detection of the [N III] λ1750 emission feature seen in component B only. In the event that the presence of the [N III] line is confirmed by future observations, it is difficult to reconcile the large difference in strength with a lensing explanation for the system, and the binary quasar hypothesis would become the favored model for the system.

4. CONCLUSIONS

Q1009−0252 is an intriguing system and origins due to gravitational lensing or a very close pair of distinct quasars both remain possibilities. The geometry, similar spectra, and existence of strong intervening Mg II absorption makes the system a strong candidate for an example of gravitational lensing by a massive galaxy. Invoking differential extinction along the two lines of sight through the lens produces a good match to the observed spectral energy distributions. However, this approach is somewhat *ad hoc* and the lens model then requires relatively large differences in the line-of-sight extinction for two very similar impact parameters. Furthermore, since the extinction cannot change the emission line equivalent widths, continuum or emission-line, variability or microlensing must be invoked to explain the differences between the spectra of A and B. Much deeper direct imaging in the I band should result in the detection, or at least place a very strict limit on the magnitude, of the $z=0.869$ absorber, providing a better understanding of the system. Further high-quality spectra of components A and B to verify the presence of the 6550 Å feature seen in component B alone will clarify whether the properties of the system present major difficulties for a gravitational lens model.

Irrespective of the interpretation for the origin of the Q1009−0252 system, absorption lines present in the three quasar spectra demonstrate that the Mg II system at $z=0.8688$ is at least $40h_{50}^{-1}$ kpc in extent and the Mg II system coincident in redshift with the $z=1.627$ quasar extends at least $45h_{50}^{-1}$ kpc from the quasar itself, providing further evidence both for the association of quasars with normal galaxies and the large spatial extent of systems responsible for strong Mg II absorption.

This research was supported in part by NSF Grants Nos. AST 90−01181 and 93-20715. A NATO Collaborative Research Grant (held by P.C.H.) aids research on gravitational lenses and quasar surveys at the Institute of Astronomy. The WHT and JKT are operated on the island of La Palma by the Royal Greenwich Observatory at the Spanish Observatorio del Roque de los Muchachos of the Instituto de Astrofisica de Canarias. Pat Osmer and Bob Carswell provided valuable help in locating papers relevant to the detection of [N III] emission.

REFERENCES

Coleman, G. D., Wu, C-C., & Weedman, D. W. 1980, ApJS, 43, 393
Djorgovski, S., Perley, R., Meylan, G., & McCarthy, P. 1987, ApJ, 321, L17
Drinkwater, M. J., Webster, R. L., & Thomas, P. A. 1993, AJ, 106, 848
Hewett, P. C., Foltz, C. B., & Chaffee, F. H. 1994 (in preparation)
Hewett, P. C., Foltz, C. B., Chaffee, F. H., Francis, P. J., Weymann, R. J., Morris, S. L., Anderson, S. F., & MacAlpine, G. M. 1991, AJ, 101, 1121
Hewett, P. C., Harding, M. E., & Webster, R. L. 1992, in Gravitational Lenses, edited by R. Kayser, T. Schramm, and L. Neiser (Springer, Heidelberg), p. 209
Hewett, P. C., Webster, R. L., Harding, M. E., Jedrzejewski, R. I., Foltz, C. B., Chaffee, F. H., Irwin, M. J., & Le Févre, O. 1989, ApJ, 346, L61
Irwin, M. J. 1985, MNRAS, 214, 575
Kochanek, C. 1993, ApJ, 419, 12
Maoz, D., Smith, P. S., Jannuzi, B. T., Kaspi, S., & Netzer, H. 1994, ApJ, 421, 34
Lanzetta, K. M., & Bowen, D. 1990, ApJ, 357, 321
Osmer, P. S. 1980, ApJ, 237, 666
Osmer, P. S., & Smith, M. G. 1980, ApJS, 42, 333
Shanks, T., & Boyle, B. J. 1994, MNRAS (in press)
Steidel, C. C. 1992, in The Environment and Evolution of Galaxies, edited by J. M. Shull and H. A. Thronson (Kluwer, Dordrecht), p. 263
Steidel, C. C., & Sargent, W. L. W. 1991, AJ, 102, 1610
Surdej, J., Remy, M., Smette, A., Claeskens, J.-F., Magain, P., Refsdal, S., Swings, J.-P., & Véron-Cetty, M. 1994, in Gravitational Lenses in the Universe; 31st Liege Int. Astroph. Coll., 1993, edited by J. Surdej, D. Fraipont-Caro, E. Gosset, S. Refsdal, and M. Remy (Universite de Liege, Liege), p. 153
Webster, R. L., Hewett, P. C., & Irwin, M. J. 1988, AJ, 95, 19